Intrinsic properties of biological motion detectors prevent the optomotor control system from getting unstable

ANNE-KATHRIN WARZECHA* AND MARTIN EGELHAAF*

Centre for Visual Sciences, Research School of Biological Sciences, Australian National University, GPO Box 475, Canberra ACT 2601, Australia

SUMMARY

Compensatory eye, head or body movements are essential to stabilize the gaze or the path of locomotion. Because such compensatory responses usually lag the sensory input by a time delay, the underlying control system is prone to instability, at least if it operates with a high gain in order to compensate disturbances efficiently. In behavioural experiments it could be shown that the optomotor system of the fly does not get unstable even when its overall gain is so high that, on average, imposed disturbances are compensated to a large extent. Fluctuations of the animal's torque signal do not build up. Rather they are accompanied by only small-amplitude jittery retinal image displacements that rarely slip over more than a few neighbouring photoreceptors. Combined electrophysiological experiments on a pair of neurons in the fly's optomotor pathway and model simulations of the optomotor control system suggest that this relative stability of the optomotor system is the consequence of the specific velocity dependence of biological movement detectors. The response of the movement detectors first increases with increasing velocity, reaches a maximum and then decreases again. As a consequence, large-amplitude fluctuations in pattern velocity, as are generated when the optomotor system tends to get unstable, are transmitted with a small gain leading to only relatively small torque fluctuations and, thus, small-amplitude image displacements.

1. INTRODUCTION

Compensatory reactions mediated by eye, head or body movements are an essential prerequisite for stabilizing the gaze or path of locomotion against disturbances. These behavioural reactions are controlled by feedback systems that, in many cases, rely on the visual system as the major source of information. Visual cues are particularly useful, because deviations from the intended path of locomotion or direction of gaze lead to characteristic displacements of the entire retinal image. These displacements are evaluated by the nervous system and exploited to generate corrective motor responses. The responses affect the retinal input and, ideally, compensate for the disturbance. In all biological systems such compensatory responses lag the sensory input with an inevitable delay. As a consequence, the feedback may cause the system to become unstable, at least, if it has to operate with a high gain in order to compensate disturbances efficiently. This means that the output of the system may get out of control and increase without bound (for review, see Land 1992).

Evolution never would have tolerated control systems that may get unstable; therefore specific strategies can be expected to be employed by nervous systems to prevent instability. Not only biological systems have to cope with the problem of instability. Also technical control systems have to be designed in a way that stability of operation is ensured. Quite generally, this can be achieved by including, in the control circuit, additional elements that reduce the overall gain when the system tends to get unstable and oscillations start to build up (e.g. Kuo 1991). In the context of compensatory eye and/or body movements this has been assumed to be accomplished by the addition of subsidiary loops to the basic control circuit. For instance, it has been proposed that a signal proportional to the motor output is fed back to the main circuit in order to control the overall gain of the system. In essence, this signal is assumed to cancel out the effect of the feedback loop before oscillations can build up (Young 1971; Robinson *et al.* 1986; Lisberger *et al.* 1987). According to another proposal, a signal proportional to retinal slip speed bifurcates from the main feedback loop and is fed into a series of a highpass filter, a rectifier and a lowpass filter. When the system starts to generate high-frequency fluctuations, the output signal of the subsidiary loop reduces the overall gain of the proposed model system and thus prevents instability (Kirschfeld 1991).

All these proposals have two features in common: (i) they rely on elements that have to be added to the basic control system; (ii) they implicitly assume,

---

* Present address: Lehrstuhl für Neurobiologie, Fakultät für Biologie, Universität Bielefeld, Postfach 10 01 31, 33501 Bielefeld, Germany.

without specifying how this might be accomplished, that the velocity of the retinal image displacements is transmitted faithfully to the optomotor controller. In the following it is shown by behavioural and electrophysiological experiments on the fly as well as by model simulations that no such additional elements are required to explain the stability of its optomotor control system, if the dynamical properties of the movement sensitive elements (Egelhaaf & Borst 1993) in the input lines of the control system are taken into account. The gain of these elements automatically decreases when the retinal velocity gets too large. The response fluctuations, which occur when the system starts getting unstable, occur with high-velocity image displacements; consequently, the intrinsic properties of the movement-sensitive elements thus ensure that the output of the optomotor control system cannot get unstable and the resulting position jitter of the retinal image stays relatively small.

2. MATERIAL AND METHODS

The experimental analysis was done with female sheepflies (*Lucilia cuprina*, Calliphoridae) that were obtained from laboratory stocks (CSIRO, Division of Entomology, Canberra).

In the behavioural experiments (§3) two CRT screens (Tektronix 608) were used for visual stimulation. The stimulus pattern was generated at a frame rate of 183 Hz by an image synthesizer (Picasso, Innisfree). Monitors were placed symmetrically at an angle of 45° with respect to the long axis and perpendicular to the horizontal plane of the fly. The angle between the screens, thus, amounted to 90°. The fly was positioned in such a way that it faced the centre of each screen with one eye at a horizontal position of 55° or $-55°$ (right and left monitor, respectively) and at an angular vertical position of 0°, with 0° referring to the frontal midline of the animal. The horizontal and vertical extent of the screens amounted to 70° and 55°, respectively. The stimulus pattern consisted of a vertical squarewave grating with five periods per screen. The mean luminance was 44 cd m^{-2}, the contrast was 0.92. The same visual stimulation set-up was used in the neuronal replay experiments where the velocity dependence of optomotor neurons in the fly's third visual neuropil was determined (§6). In the neuronal closed-loop experiments (§5) a single CRT screen was placed symmetrically directly in front of the fly. Its horizontal and vertical extent amounted to 72° and 57°, respectively. Eight periods of a squarewave grating with a contrast of 0.99 and a mean luminance of 16 cd m^{-2} were displayed on the screen. In both the behavioural as well as the electrophysiological experiments, the pattern parameters, such as spatial wavelength and contrast, were chosen as to elicit strong responses because in the closed-loop situation these are accompanied with a high gain and may thus be most critical with respect to the stability of the optomotor control system.

(*a*) *Behavioural experiments*

Behavioural experiments were performed with a torque meter that allows the measurement of the fly's compensatory optomotor turning responses while the animal is flying stationarily in space (Fermi & Reichardt 1963; Götz 1964). The fly was glued to a triangular piece of cardboard. With this cardboard triangle the fly could be fixed to the torque meter. The torque meter was operated under closed-loop conditions, i.e. the animal's yaw torque response was fed back to the visual stimuli in basically the same way as under natural flying conditions. This feedback was achieved by reading the torque signal into a computer that calculated the visual consequences of the fly's actions and reactions and modified the visual input accordingly (figure 1*a*). This system, thus, formed a kind of computer–behavioural hybrid. The torque signal was sampled at a frequency of 400 Hz by a 12-bit analog-to-digital converter of an I/O card (2801A, Data Translation) plugged into a 486 PC. This signal was transformed into image motion in the following way. The position of the stimulus pattern was controlled via the image synthesizer with a seven-bit resolution for the spatial phase of the grating. Every 2.5 ms a seven-bit signal was sent from the computer via the digital port of the I/O card to the external phase input of the image synthesizer. This output signal displaced the grating depending on the external motion bias as well as on the amplitude and sign of the momentary torque. For some time during the experiments an external motion bias was added to the input of the control system that, under open-loop conditions, would have displaced the stimulus pattern with a constant velocity. The torque signals and the time during which an external motion bias was imposed were stored. Thus, it was possible in the electrophysiological experiments to replay the same time-dependent motion traces that were generated under behavioural closed-loop conditions. This procedure was used previously to replay those stimuli in behavioural open-loop experiments that were generated beforehand under behavioural closed-loop conditions (Heisenberg & Wolf 1988). As in previous studies (e.g. Reichardt 1973; Reichardt & Poggio 1976; Heisenberg & Wolf 1984; Heisenberg & Wolf 1988) the image motion induced by the fly's own actions and reactions was controlled in such a way that the yaw torque was proportional to the resulting pattern velocity. A 'coupling coefficient' was chosen which led to an angular pattern velocity of 10.8° s^{-1} for a torque of 1×10^{-8} Nm. Basically the same results as those reported here were obtained for a wide range of coupling coefficients (M.E. and A.-K.W., in preparation; see also Wolf & Heisenberg 1990). The torque signal was lowpass filtered with a cutoff at 5 Hz. This cutoff frequency was chosen because it is well below the resonance frequency of the torque meter and its associated electronics. However, it was confirmed in control experiments that the characteristic features of the behavioural responses did not change qualitatively when the cutoff was set to either 10 or 2 Hz. Before data acquisition could start, the zero torque level had

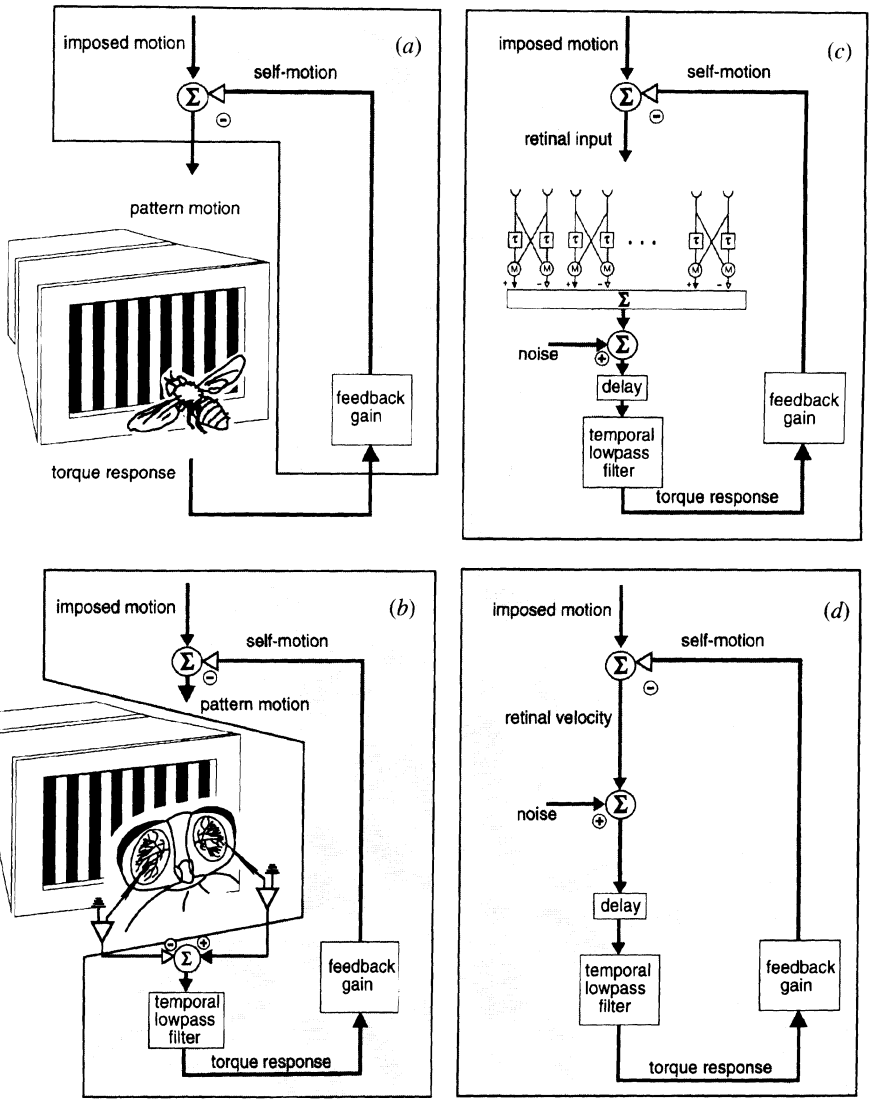

Figure 1. Control circuits approximating the fly's optomotor system. The circuits differ in the extent that is simulated on a computer (shaded areas in the diagrams). (*a*) Computer–behavioural hybrid: A flying fly is the centre of the control circuit. The fly is tethered to a torque compensator (not shown) that allows measurement of its instantaneous torque. In contrast to free flight, the torque signal generated by the fly does not lead to turns of the animal that normally would induce retinal image displacements. Rather the visual consequences of self-motion are simulated by feeding the torque signals into a computer and transforming them into image displacements on a CRT screen (for convenience, only a single screen is shown, whereas in the behavioural closed-loop experiments two screens were used, one in front of either eye; see §2). The image displacements are assumed to be proportional to the torque; their amplitude depends on the gain of the feedback loop. In addition to the self-induced image displacements, an additional motion bias can be imposed on the optomotor control system. (*b*) Computer–neural hybrid: The torque responses of the flying fly are substituted by the simultaneously recorded spike responses of a pair of optomotor neurons, the H1 cells, in both halves of the brain followed by a subtraction stage and a temporal lowpass filter (first order; time constant: 750 ms). The output of this filter is assumed to correspond to the torque response and to control the visual input of the system in the same way as described in (*a*). (*c*) Model circuit: the pattern motion on a real monitor as well as the optomotor neurons is substituted by simulated pattern motion that is fed into an array of correlation-type movement detectors, the output of which is spatially integrated and delayed. Hence all the components of the control circuit are modelled. The brightness values of the changing retinal image were processed by equidistant movement detectors that were stimulated by a sinewave grating. For the sake of clarity adjacent movement detectors were drawn separately although they share one input line. Each detector consists of two mirror-symmetrical subunits. In each subunit, one of the input signals is lowpass filtered (τ) and multiplied (M) with the unfiltered signal of the adjacent input channel. The output signals of an array of movement detectors are summed, with the two mirror-symmetrical subunits contributing with either a positive (filled arrowheads) or negative sign (open arrowheads) to the overall response. Then the noise is added to the signal which, after a delay, is fed into a lowpass filter (first order; time constant: 750 ms). The delay amounts to either 60 or 75 ms depending on whether the behavioural or neuronal closed-loop performance is simulated. As in (*b*), the output of this filter is assumed to correspond to the torque response. This signal leads, via a feedback loop, to displacements of the simulated visual surround and thus to changes in the simulated retinal input. (*d*) As (*c*) without correlation-type movement detectors. The retinal input of this standard linear control circuit corresponds to the velocity of the pattern.

to be adjusted. An estimate of the zero torque level was obtained by time-averaging, under closed-loop conditions, the fly's responses for one minute while an external motion bias was applied to the pattern which alternated between clockwise and counterclockwise rotation every five seconds. Because the mean torque determined in this way sometimes drifted to other levels, this computer-controlled procedure for determining the zero torque level was repeated after every ten sweeps of data acquisition (for details, see Warzecha 1994). ASYST (Keithley Instruments) was used as a programming language for data acquisition and evaluation. One thousand and twenty-eight sweeps of 19 flies, in total, were recorded. A considerable amount of variability was found in the responses. One end of this range is characterized by slow changes of the torque that may last for several seconds and do not show any obvious relation to the motion stimulus. The other end of the variability range is represented by responses that lead to a good compensation of the external motion bias and thus reflect a high internal gain of the system. In these traces there is a tendency towards periodic fluctuations around the mean response level (see §3). Because a linear feedback control system exhibiting this kind of oscillations is on the brink of instability, these response traces are particularly important in the present context. Therefore, 139 of these sweeps were selected for further analysis and used as stimuli in electrophysiological experiments in which the velocity dependence of an optomotor neuron was determined.

(*b*) *Model simulations*

Model simulations of the optomotor control system were performed on a 486 PC using ASYST as the programming language. The main features of the model control system are outlined in §4 (figure 1*c*). The parameters were chosen to lie within a physiologically plausible range and fit the stimulus conditions of the corresponding experiments. Analogous to the optomotor neurons in the third visual neuropil that pool the signals of many local motion sensitive neurons, in the model the output of a one-dimensional array of correlation-type movement detectors was spatially integrated (Egelhaaf *et al.* 1989). The movement detectors consisted of two mirror-symmetrical subunits that shared the same two input lines. Each subunit was composed of two branches, one of which was equipped with a first-order lowpass filter (time constant: 52.5 ms; see Ruyter van Steveninck *et al.* 1986; Borst & Egelhaaf 1987; Egelhaaf & Reichardt 1987). The signals of both branches were multiplied within a subunit. The output signals of an array of movement detectors were summed, with the two subunits contributing with either a positive or negative sign to the overall response (for review, see Borst & Egelhaaf 1989). The angular separation of the two input lines of the detectors was set to 2.3°. Although the exact detector spacing is not known for *Lucilia*, this is likely to be within the same range as for *Musca* (2°: Pick & Buchner 1979) and *Calliphora* (1.2–2.3°, depending on the eye region: Franceschini *et al.* 1979). Based on the experimental results of the present study, the delay of the model torque was set to 75 or 60 ms when behavioural or neuronal responses, respectively, were simulated. Gaussian noise was added to the signal after the spatial integration stage. As a first approximation to a temporal integration stage in the optomotor control system (Egelhaaf 1987; Wolf & Heisenberg 1990), a first-order lowpass filter was implemented with a time constant of 750 ms (see Warzecha 1994). The feedback gain was adjusted as specified for the various model simulations in the corresponding figure legends. In addition simulations of a standard linear model circuit were performed (§5). Here the movement detectors in the input lines of the optomotor control circuit were omitted and the input to the lowpass filter assumed to be proportional to pattern velocity (Figure 1*d*).

(*c*) *Electrophysiological experiments*

For electrophysiological experiments the animals were dissected as described previously (Warzecha *et al.* 1993). In brief: after the head capsule was opened, the brain was supplied with Ringer's solution (for composition, see Hausen 1982*a*) to avoid desiccation. Electrolytically sharpened tungsten electrodes insulated with varnish were used to record extracellularly from the H1 cell, a spiking neuron in the optomotor pathway that can be identified individually in different flies (Hausen 1981). The electrodes had resistances between 2 and 8 MΩ. Recorded signals were amplified by standard electrophysiological equipment. The spikes were transformed into pulses of fixed height and duration that were fed to the computer through the same I/O card as was used in the behavioural experiments. In the neuronal closed-loop experiments (figure 1*b*; see §5) the H1 cells in both halves of the brain were recorded simultaneously in their telodendritic regions. The signals were sampled at a frequency of 800 Hz. The spike count in consecutive time bins obtained from the left neuron was subtracted from the spike count in the corresponding time bins obtained from the right cell. The resulting difference signal was temporally lowpass filtered in exactly the same way as the summed movement detector output in the model simulation (see above) and then used via a feedback loop to control the visual stimulus. This was done in the same way as described above for the behavioural closed-loop experiments. The coupling coefficient for this computer–neural hybrid was varied as described in §5. In the experiments where the velocity dependence of the H1 neuron was determined the data were sampled at a frequency of 1.2 kHz and evaluated in a conventional way as detailed in §6.

3. BEHAVIOURAL ANALYSIS OF OPTOMOTOR COURSE STABILIZATION

The performance of tethered flying flies in stabilizing their flight course was analysed with the computer–behavioural hybrid. The mean response to 139 stimulus presentations obtained from five flies is shown in figure 2*a*. After the spontaneously generated torque was recorded for 7.5 s (only the last 3.75 s of which are

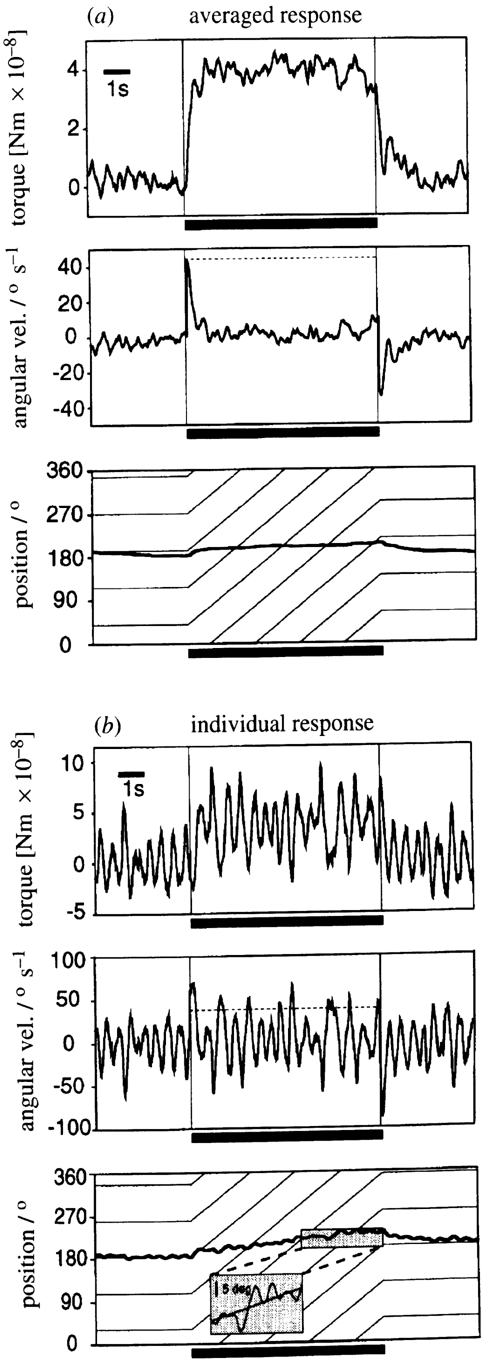

Figure 2. Averaged (*a*) and individual (*b*) behavioural responses to motion and their visual consequences as determined on the basis of the optomotor control circuit shown in figure 1*a*. For a duration of 7.5 s (indicated by the bars underneath the diagrams) an external motion bias with a constant velocity of 44° s^{-1} was added to the pattern displacements induced by the fly's own torque. Upper traces: torque response in a closed-loop situation. Middle traces: corresponding retinal angular velocity of the pattern; the open-loop velocity is indicated by a dashed horizontal line. Bottom traces: angular position of the pattern. The angular positions that five arbitrarily chosen pattern elements would assume in an open-loop situation are indicated by thin lines. As the size of the monitor screens was limited not all of these pattern elements are visible at all times. Note that the origin of the ordinate scale is arbitrary for a periodic pattern. One section of the unaveraged position trace is expanded. The straight line through this section indicates the mean time-dependent angular position as determined from the average angular velocity for the time interval shown by the inset. Averages shown in (*a*) are obtained from 139 responses of five flies.

displayed in figure 2*a*) an external motion bias was added for another 7.5 s to the signal generated by the fly itself. If the torque signal had not been fed back to the visual stimulus ('open-loop' conditions), this imposed motion bias would have displaced the stimulus pattern with a constant velocity of about 44° s^{-1}. (The exact velocity depends on the location on the screen due to perspective distortion.) Following the time interval with imposed motion bias the spontaneous activity was recorded again for 3.75 s. Without external motion bias flies are expected to turn equally often to the left and to the right. Therefore, on average, flies should not induce displacements of the stimulus pattern during this time. These expectations are confirmed to a large extent, as is shown for the averaged responses in figure 2*a* (middle and bottom panels). However, a slight drift of the pattern can be discerned during the time without motion bias. This apparent asymmetry is most likely due to the variability of behavioural responses (Warzecha 1994) and the limited sample of flies that were included in the average. When an external motion bias is added, flies generate a torque signal that, after a brief transient phase, compensates most of this motion bias (difference in mean slip speed before and during motion bias: 9.4% of the corresponding open-loop velocity). Accordingly, the angular position of the pattern does not change very much. After the imposed motion bias stops, flies, on average, stop generating the compensatory torque response. Consequently, the mean slip speed, after a brief transient, returns to the value it assumed before the motion bias was added. The onset of the recorded torque response lags the onset of the motion bias by 75 to 90 ms. It should be noted that about 25 ms of this delay have to be attributed to the torque compensator and the subsequent electronic system.

In contrast to the average performance of the computer–behavioural hybrid, the unaveraged torque signals are characterized by pronounced fluctuations over time (figure 2*b*). Similar torque fluctuations have been described previously for *Drosophila* (Mayer 1989; Wolf & Heisenberg 1990). To characterize the fluctuations of the unaveraged responses, the spectral density of each of the 139 response traces was calculated. The mean power density spectrum resulting from averaging these spectral densities reveals a distinct peak at about 2 Hz (figure 3). The shape of the power density spectrum does not depend much on the cutoff frequency of the compensator electronics. Merely the peak was found to shift to slightly higher or lower values, when the cutoff frequency was set to 10 or 2 Hz, respectively. The existence of this peak illustrates that there is a strong periodic component in the response traces. Hence, it is suggested that the fluctuations do not simply represent noise.

What are the visual consequences of the pronounced torque fluctuations? To answer this question the slip speed and the corresponding angular position of the stimulus pattern were plotted as a function of time (figure 2*b*, middle and bottom diagram). The slip-speed fluctuations are very pronounced both during time intervals with and without external motion bias. With a standard deviation of 35.8° s^{-1} determined for

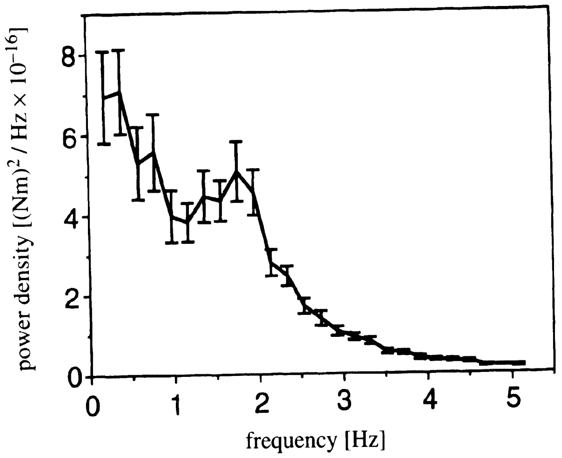

Figure 3. Mean power density spectrum of torque responses to an imposed motion bias. Power spectra were calculated by a fast Fourier algorithm. Responses within a time interval of 5.12 s starting 2.38 s after the onset of the imposed motion bias were taken into account. This interval length was chosen because it corresponds to a number of data points amounting to an integral power of two, the number required for the fast Fourier algorithm. The average contribution of each frequency component and its associated standard error of the mean are shown for a range of frequencies between 0.2 and 5.1 Hz. The power density spectrum was scaled so that the total power equals the variance of the corresponding response traces (in (Nm)^2). The same data set was used as in figure 2.

2.5 ms bins during the last 3.2 s of the time with motion bias, the time-dependent retinal pattern velocity is almost as large as the open-loop velocity. During the time with external motion bias, the pattern slowly drifts to the right, because the fly does not perfectly compensate the external disturbance. This drift is small compared to the displacements expected in an open-loop situation as is indicated by the oblique lines. The inset in figure 2*b* (bottom diagram) shows, on an enlarged scale, the fluctuations around the time-dependent position (straight line in inset) that the pattern would have assumed if it were displaced with the mean slip speed within the time interval shown in the inset. To quantify the size of these fluctuations their standard deviation from this mean time-dependent pattern position was determined for all 139 response traces. This was done for 2.5 ms bins during the last 3.2 s with an imposed motion bias. On average, the fluctuations around the mean pattern displacement amount to 7.8°. Hence, the large torque and slip-speed fluctuations are not accompanied by large displacements from the mean flight course.

4. BEHAVIOURAL PERFORMANCE CAN BE MIMICKED BY A CONTROL SYSTEM WITH CORRELATION-TYPE MOVEMENT DETECTORS IN ITS INPUT LINES

Several conclusions can be drawn from the behavioural analysis of the optomotor system of the fly: (i) flies are able to compensate for most of an imposed disturbance by optomotor torque responses; (ii) they generate torque fluctuations that contain a strong periodic component. Under open-loop conditions no periodic component can be discerned in the torque traces (Heisenberg & Wolf 1988, M.E. and A.-K.W., unpublished results); consequently, it is suggested that they are the consequence of a high feedback gain in the closed-loop situation; (iii) the position jitter of the stimulus pattern stays small and does not much affect the stabilization of the retinal image.

How can these distinguishing features of the fly's optomotor system be explained? The impressive compensatory behaviour of the fly is most likely due to the action of an optomotor course control system most sensitive to extended moving patterns rather than to a fixation system sensitive to the position of edges (Heisenberg & Wolf 1984). In the first step of the analysis, it was therefore tried to simulate the behavioural performance on the basis of a model of the optomotor control system (figure 1*c*). The input signal of the model consisted of a sinewave grating which was moved according to the difference between the retinal image displacements induced by externally imposed motion and the displacements resulting from the model fly's own torque response. The retinal image motion was sensed by an array of correlation-type movement detectors. This type of movement detectors was included in the model circuit, because it has been shown in many studies that it can account for the major characteristics of the fly's motion detection system (for review, see Egelhaaf & Borst 1993). The outputs of the movement detectors were summed, because optomotor responses can be elicited within large parts of the visual field. This processing stage is assumed to correspond to the spatial pooling of local motion signals by the dendritic tree of the optomotor neurons in the third visual neuropil (Egelhaaf *et al.* 1989). The summed detector output was fed into a temporal lowpass filter as an integrating element and transformed into the torque signal. An integrating element in the optomotor control system of the fly has previously been concluded to exist on the basis of behavioural experiments (Egelhaaf 1987; Wolf & Heisenberg 1990). A time delay was included into the model because the fly's torque response lags the retinal input. This was done here, quite arbitrarily, after the spatial integration stage. It should be noted that it does not matter, with regard to the performance of the control system, where the delay element is located in the circuit. The gain of the system was chosen so as to lead to a residual retinal slip speed during the time interval with an external motion bias (13.5% of the motion bias) that was within the range found in the corresponding behavioural experiments (9.4%, see §3). It has been found that the stochastic signal fluctuations, intrinsic to the elements of the optomotor pathway are essential to account for the performance of the optomotor control system (Warzecha 1994); thus Gaussian noise was added to the output of the spatial integration stage (for details of noise amplitude see the legend of figure 4).

When the model parameters were set as estimated on the basis of the available experimental data (see §2 and the legend of figure 4), the model responses were very similar to the corresponding behavioural results (compare figures 2 and 4).The mean displacements of the stimulus pattern are slightly smaller in the behavioural than in the model responses, only during the time with motion bias. This difference is essentially a consequence of the small drift of the pattern in the opposite direction to the motion bias as found in the behavioural experiments (see Section 3). Not only the averaged but also the individual response traces look very similar to the corresponding experimental data. In the model, the standard deviation of the slip-speed fluctuations was 37.7° s^{-1} compared to 35.8° s^{-1} for the behavioural–computer hybrid. They occur with position fluctuations around the mean pattern displacements with a standard deviation of 6.3° (vs. 7.8° for the behavioural–computer hybrid). Similar to the experimental results, there is also a strong periodic component in the model torque response traces. This close correspondence between the main features of the behavioural responses and of the model output holds for a wide range of coupling conditions (A.-K. W. and M. E., unpublished results). This suggests that the feedback control circuit as outlined here is a fairly good representation of the fly's optomotor control system.

5. MOVEMENT DETECTORS ENSURE STABILITY OF OPTOMOTOR CONTROL SYSTEM

A standard linear control circuit would operate on the brink of instability when it performs in a similar way as described above for the computer–behavioural hybrid and the model shown in figure 1*c*, i.e. when its output signal fluctuates strongly while disturbances are, on average, compensated well. However, instability was never observed for the latter control systems. The reasons for this observation were systematically investigated by the following two procedures: (i) for a large range of feedback gains the performance of a model control circuit equipped with correlation-type movement detectors in its input lines (figure 1*c*) was compared to that of a standard linear optomotor control circuit for which the torque is proportional to pattern velocity (figure 1*d*); (ii) the motion detection stage of the model with correlation-type movement detectors was replaced by a pair of corresponding optomotor neurons in the right and left optic lobe (compare figure 1*c* and *b*). The activity of

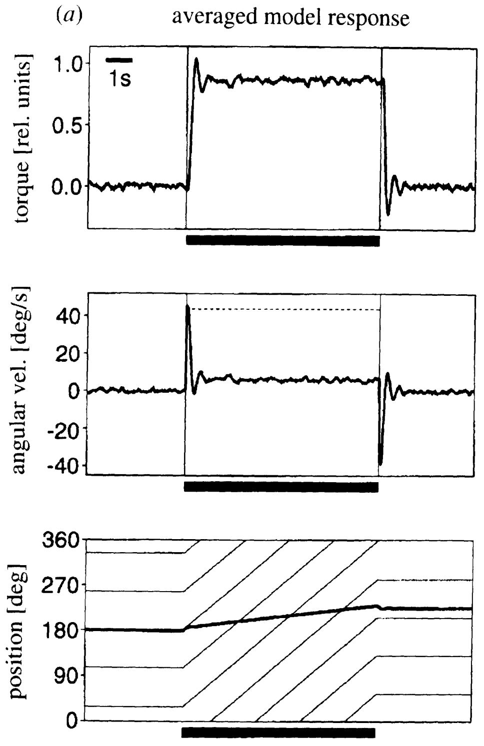
(*a*) averaged model response

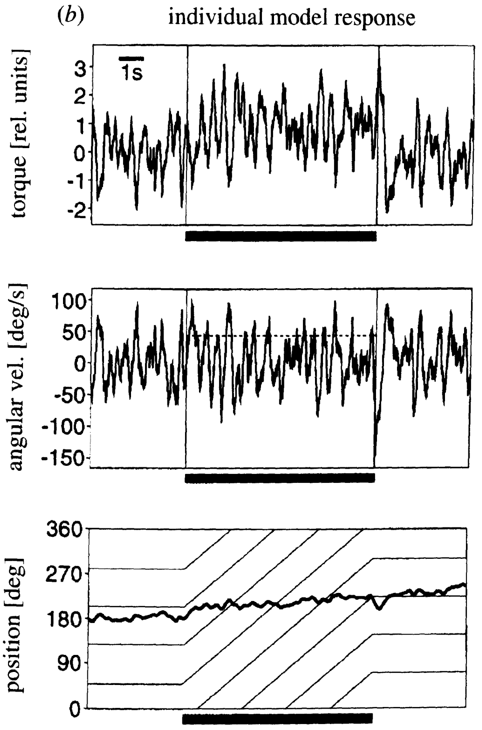
(*b*) individual model response

Figure 4. Model simulation of the performance of the optomotor system (circuit diagram of model shown in figure 1*c*): (*a*) averaged responses; (*b*) example of an individual response trace. The stimulus situation is analogous to that of figure 2. The bars underneath the diagrams illustrate the duration of the external motion bias. Upper traces: torque response in a closed-loop situation. Relative units are scaled so that a value of one leads to a perfect compensation of the imposed motion bias. Middle traces: corresponding retinal slip speed; the open-loop velocity is indicated by dashed horizontal line. Bottom traces: angular position of the pattern. The angular positions that five arbitrarily chosen pattern elements would assume in an open-loop situation are indicated by the thin lines. Not all of these pattern elements were within the receptive field of the movement detector array at all times. Note that the origin of the ordinate scale is arbitrary for a periodic pattern. Averages shown in (*a*) are obtained from 3000 simulated responses. Gaussian noise was added to the output of the spatial integration stage. The noise was adjusted so that the time course and the amplitudes of the fluctuations of the model response were in accordance with the corresponding experimental results. The noise had a standard deviation of 16 times the mean torque response. The basic time step used in the simulations was 15 ms. A time delay of 75 ms was included in the circuit to approximate the experimentally determined latency. The feedback gain was adjusted in such a way that the difference in the mean simulated slip speed before and during the motion bias came close to the increase in retinal slip speed as determined in the corresponding behavioural experiments. Six detectors covered exactly one pattern wavelength of 14°. The imposed motion bias amounted to 44° s^{-1}.

these neurons was allowed to control the stimulus, while the gain of the feedback loop was varied. The properties of this computer–neural hybrid with respect to its stability were investigated and compared to that of the models. The performance of these different versions of the optomotor control circuit has been assessed by determining the residual mean slip velocity and the position error during an imposed motion bias for various feedback gains. The position jitter was calculated as detailed in §3 for the behavioural closed-loop experiments.

The model control circuit with correlation-type movement detectors (figure 1*c*) was simulated in basically the same way as outlined in §4. For the linear optomotor control circuit the movement detectors in the input lines were omitted and the input signal was assumed to be proportional to velocity (figure 1*d*). For the sake of comparison, the parameters for both models were chosen to match the experimental conditions used for investigating the properties of the computer–neural hybrid (see below). The feedback gain that leads to a compensation of the imposed motion bias to 70% of the open-loop velocity was arbitrarily set to one. Further details are given in the legend of figure 5*a*. The standard linear control circuit (figure 1*d*) gets unstable when the feedback gain surpasses a given limit (figure 5*a*, unstable within shaded area). Up to this limit the mean slip speed decreases with increasing gain, whereas the position jitter, being small for small gains, increases slightly. The model of the optomotor system with correlation-type movement detectors in its input lines (figure 1*c*) performs almost identically to the standard linear control circuit (figure 1*d*) within the stability range of the latter (compare open and filled symbols in figure 5*a*). However, above the critical limit it does not get unstable. Only the mean slip speed now tends to increase while the position error keeps growing with increasing feedback gain. Because both model circuits differ from one another only by the way in which motion information is processed, it seems likely that the properties of the motion detection stage are essential for the stability of the system. In the following it will be tested whether this holds also for biological movement detectors.

The consequences of the properties of the fly's motion detection system on the stability of the optomotor control circuit were tested by substituting a pair of corresponding optomotor neurons in both halves of the brain for the correlation-type movement detectors of the model (compare figure 1*b* and *c*). For this purpose the computer–neural hybrid was preferred to the computer–behavioural hybrid because, in this way, the influence of nonlinearities after the motion detection stage on the stability of the system can be excluded. In the experiment the activity of a pair of individually identifiable intrinsic neurons of the fly's optomotor system, the motion-sensitive H1 neurons (Hausen 1981) was recorded simultaneously. The H1 neurons exist once in each half of the brain and respond to back-to-front motion within the visual field of one eye. In corresponding time bins of 1.25 ms duration, the responses of the two H1 cells were subtracted from each other (figure 1*b*). To account for the properties of the optomotor system, the difference signal was fed into a temporal lowpass filter as has been done for the model simulations after the motion detection stage. The output of this filter was fed back to the visual input of the system in the same way as in the behavioural closed-loop experiments (see §3). As for the model simulations the performance of this computer–neural hybrid, in terms of residual slip speed and position jitter, was assessed for various gains of the feedback loop. The smallest feedback gain that was used in the experiments led to a reduction of the average slip speed to 70% of the open-loop velocity and was set to one. As is shown as an example in figure 5*b*, the mean slip velocity first decreases with increasing feedback gain. However, above a certain coupling strength it tends to increase again. For small feedback gains the position jitter is small. It increases with increasing feedback gain. Note, however, that until a gain of 100 is reached it is smaller than 1.5° and, thus, smaller than the angular distance between neighbouring photoreceptors. The position error increases to higher values only when the feedback gain increases further. It should be noted, that a feedback gain of 100 is already extremely high as a single spike leads to a pattern displacement of 7°. Owing to the lowpass filter in the optomotor system, this displacement is not executed instantaneously but has a time course according to the impulse response of the filter. The difficult experiment with the computer–neural hybrid that requires stable simultaneous long-term recordings of two cells was done for the whole range of feedback gains in two flies with qualitatively the same results.

Thus, the performance of the computer–neural hybrid qualitatively resembles that of the model circuit with correlation-type movement detectors. In contrast to the standard linear model circuit, both systems do not get unstable, even though they do not contain any of the elaborations proposed previously (see §1). When the feedback gain is sufficiently high to lead to a good compensation of an imposed motion bias, signal fluctuations occur. However, the resulting position jitter is rather small.

Although the performance of the computer–neural hybrid can be accounted for qualitatively by an optomotor control circuit with correlation-type movement detectors in its input lines, there are quantitative differences (compare figures 5*a* and *b*). These are likely to be due to several reasons: (i) the noise fed into the control circuit was characterized by a constant standard deviation, although the stochastic signal fluctuations in fly optomotor neurons depend to some extent on the activity level of the cell (Warzecha 1994). It should be noted that the noise amplitude required to mimic the time course of the behavioural responses under closed-loop conditions (§4) was considerably larger than the noise used in the models of the computer–neural hybrid (§5). Accordingly the position jitter obtained in the simulations of the computer–behavioural hybrid was larger than that found in the neuronal closed-loop experiments and corresponding simulations; (ii) first-order lowpass filters were used in the model movement detectors, although it is likely that the details of the properties of fly motion detectors can be approximated much better with higher order filters or combinations of different temporal filters in both branches of each movement detector subunit; (iii) the time constant of the movement detector filter was assumed to be constant, although there is experimental evidence that it can adapt to the prevailing stimulus conditions (see Ruyter van Steveninck *et al.* 1986; Borst & Egelhaaf 1987). It should be noted, however, that it has not been the main purpose of the model simulations shown here to fit all the details of motion detector responses as closely as possible. Rather it was intended to show that correlation-type movement detectors even in their basic form without any elaborations suffice to prevent the optomotor control circuit from getting unstable.

6. VELOCITY DEPENDENCE OF MOVEMENT DETECTORS UNDER TRANSIENT CONDITIONS

Why does the optomotor control system of the fly not get unstable, despite the fact that the motor output lags the sensory input by a time-delay? According to the

(*a*) model simulation

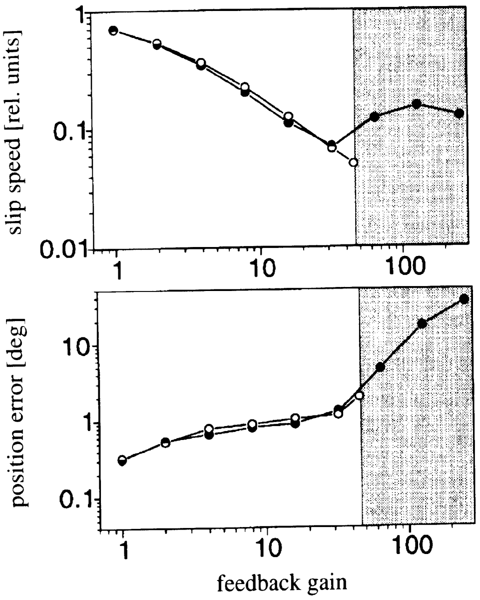

(*b*) computer–neural hybrid

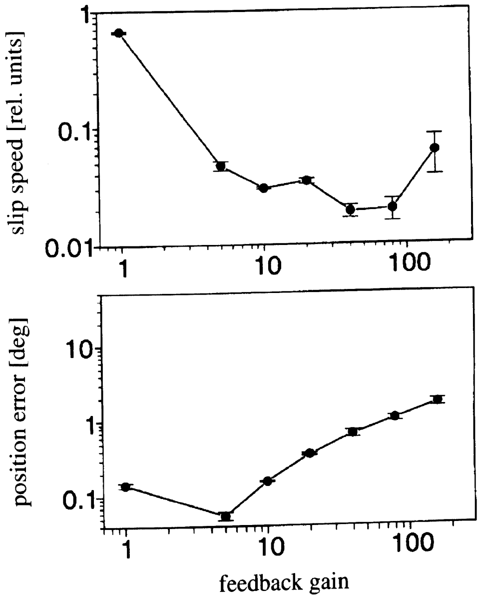

Figure 5. Residual slip speed (upper diagrams) and position error (bottom diagrams) of optomotor control circuits under closed-loop conditions during an imposed motion bias as a function of the feedback gain. The position error is given by the standard deviation of the instantaneous pattern position from the time-dependent position that the pattern would assume if it were displaced at a constant rate with the mean slip speed. The residual slip speed was normalized with respect to the open-loop velocity of the imposed motion bias. (*a*) Model simulations of the optomotor control system. The performance of a standard linear control circuit (open symbols, see figure 1*d* for the circuit diagram) is contrasted with the properties of the control system with correlation-type movement detectors in its input lines (closed symbols; see figure 1*c* for the circuit diagram). The linear control circuit implicitly assumes perfect velocity sensors in its input lines. The feedback gain that reduces the motion bias to 70% was arbitrarily set to one. For the feedback gains indicated by the shaded area the linear control system is unstable. The time step used in these simulations was 2.5 ms. This fine temporal resolution was used to avoid aliasing which may be critical for large gains that may result in large angular velocities of the pattern. The mean slip speed and position error of the model were repeatedly determined for intervals of 20 s during a maintained motion bias of 18° s^{-1}. This was done until the values of the mean slip speed and position error virtually did not change any more. Four detectors covered one spatial pattern wavelength of 9.3°. A time delay of 60 ms was included in the circuit to approximate the experimentally determined phase shift (see Section 6). Moreover, Gaussian noise was added before the responses were temporally lowpass filtered. The standard deviation of the noise was adjusted to its experimentally determined counterpart in the following way. The neuronal noise, given by the standard deviation of the individual response traces from the averaged response trace, as determined in electrophysiological replay experiments (see Warzecha 1994) was used as reference. To be able to relate the neuronal noise to the model noise, both were normalized with respect to the corresponding mean response amplitude of the closed-loop response with a feedback gain of one. If the neuronal noise was evaluated at the same temporal resolution as was used in the model simulations (2.5 ms per time step), its standard deviation amounted to 1.45 times the mean response amplitude obtained with gain one. (*b*) Neuronal closed-loop experiments (see figure 1*b* for the circuit diagram). The difference of the spike count of the two H1 cells in both halves of the brain was computed and fed into a temporal lowpass filter. The output of this filter controlled the pattern motion on a CRT screen. The time constant of the lowpass filter was identical to that used in the simulations, i.e. 750 ms. It was ensured that the pattern displacements between consecutive frames were considerably less than half the pattern wavelength preventing aliasing effects. The elementary time step was 1.25 ms. During the first 7.5 s of an experiment no external motion bias was imposed and all pattern displacements resulted from the activity of the H1 cells. In the following 10 s a motion bias of 18° s^{-1} was added (further details, see text). The residual slip speed was determined by averaging the slip speed during the last 5 s of the time with imposed motion bias. Error bars denote SEMs calculated on the basis of three to six experiments performed with one fly.

results presented in Section 5, stability of the fly optomotor system is ensured by the characteristic properties of the movement detectors in its input lines. As correlation-type movement detectors the movement detectors in the fly visual system do not lead to a faithful representation of pattern velocity (e.g. Egelhaaf & Reichardt 1987). Most conspicuously, the mean response amplitude increases with increasing velocity, reaches a maximum and then decreases again (Hausen 1982*b*; Maddess & Laughlin 1985). Hence, the gain of the movement detection system depends on pattern velocity in a nonlinear way. To test whether these results, obtained by moving a pattern with a constant velocity, also hold for the highly transient retinal displacements (as are characteristic of optomotor course control under closed-loop conditions), the H1 neuron in one half of the brain was successively confronted under open-loop conditions with all the 139 stimulus traces that were generated by the fly in the behavioural experiments and were included in the averaged response shown in figure 2*a*. In order to determine the velocity dependence of the optomotor neuron, the instantaneous neuronal response was related to the velocity of that stimulus by which it was elicited. Here the time shift between stimulus and response had to be taken into account. This time shift was determined by cross-correlating the velocity and the corresponding time-dependent spike-frequency histogram as determined from the responses elicited by presenting the same motion trace 60 times. The cross-correlogram had a maximum at 60 ms. Therefore, the number of spikes within bins of 10 ms were calculated and related to the corresponding velocity signal averaged over a 10 ms interval occurring 60 ms earlier. The exact size of the time interval does not affect the results qualitatively, as has been confirmed for time intervals of up to 40 ms.

The velocity dependence of the H1 cell is shown in figure 6*a*. The response increases almost linearly with velocity up to about 30° s^{-1}. For larger velocities the response reaches a maximum and then decreases again. Hence, in this respect the gain of the movement detection system depends on the pattern velocity in a similarly nonlinear way for stationary and transient stimulus conditions. It should be noted, however, that the response amplitude of fly optomotor neurons does not only depend on pattern velocity but also on higher-order temporal derivatives of the pattern displacement (Egelhaaf & Reichardt 1987). The relationship between velocity and neuronal response depicted in figure 6*a* should, therefore, not be taken as a characteristic curve that allows the prediction of a neuronal response amplitude from a given velocity. The velocity dependence of the correlation-type movement detectors that were used for the model simulations in §4 was determined in basically the same way as described above for the optomotor neuron on the basis of the motion traces that were obtained under closed-loop conditions. As is illustrated by figure 6*b* the resulting curve has the same principal features as the corresponding experimental data (for possible reasons of quantitative differences, see the last paragraph of §5): the model response first increases with increasing velocity, reaches a maximum and then decreases again. Hence, in contrast to a control system with perfect velocity sensors, the gain of the motion detection system in the fly's optomotor pathway is not constant, but becomes small at high velocities.

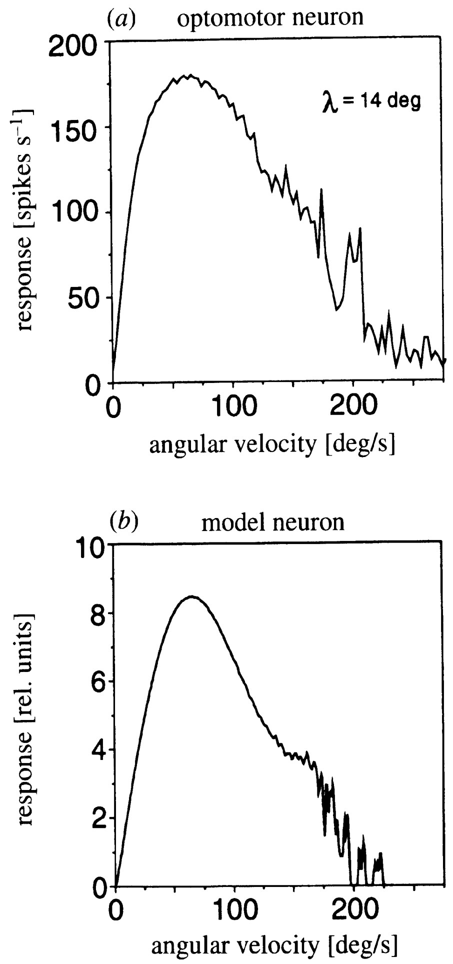

Figure 6. Velocity dependence of the responses of a neuron in the fly's optomotor system (H1 cell) (*a*) and of the summated responses of an array of correlation-type movement detectors in the model circuit shown in figure 1*c* (*b*). The neuronal responses were elicited by the 139 stimulus sequences that were generated by flies at the torque compensator under closed-loop conditions and that led to the average response shown in figure 2*a*. The temporal shift between the slip speed and the H1-cell response was determined by cross-correlation to be 60 ms. The velocity dependence was obtained by measuring the number of spikes within 10 ms bins and by relating these numbers to the velocity within 10 ms bins occurring 60 ms earlier. The velocity dependence of the model (see figure 1*c* for the circuit diagram) was obtained from 3000 simulated response traces in an equivalent way to the corresponding electrophysiological experiment. Parameter settings are identical to those of the model discussed in §4. Scaling of velocity and model responses are as in figure 4.

7. DISCUSSION AND CONCLUSIONS

The real-time performance of tethered flying flies in compensating external disturbances under closed-loop conditions can be explained quite well by a rather simple model of optomotor course stabilization. This model consists of an array of biologically plausible movement detectors whose output is lowpass filtered and fed back to the visual input. Moreover, a noise source had to be included in order to account for the temporal fine structure of the behavioural responses. By combining behavioural and electrophysiological experiments with model simulations, it could be shown that the optomotor control system of the fly cannot get unstable even for very high feedback gains. This important feature of the optomotor control system is concluded to be the consequence of the characteristic velocity dependence of the motion detectors in its input line (see also Varjú 1973). In particular, because the gain of the movement detectors decreases for large pattern velocities as are generated when the optomotor system tends to get unstable, these are transmitted only weakly to the subsequent processing stages and thus lead to only relatively small torque responses. As a consequence, torque fluctuations cannot build up and the system stays relatively stable. Thus, the implementation of additional elements in subsidiary loops of the optomotor control circuit, as has been proposed to reduce the overall gain of the system and thereby to ensure their stability (Young 1971; Robinson *et al.* 1986; Lisberger *et al.* 1987; Kirschfeld 1991), appears superfluous.

The movement detectors in the input lines of the optomotor control circuit are not the only elements in the fly's motion pathway that may reduce the gain of the system at high velocities. Already the most peripheral elements in the fly's visual system such as the photoreceptors and the large monopolar cells in the first visual neuropil do not transmit high-frequency temporal contrast modulations as occur at high pattern velocities (for review, see Laughlin 1981). It should be noted, however, that the high-velocity cutoff of these peripheral elements is, for a given spatial pattern wavelength, at much higher velocities than those of the movement detectors (compare e.g. Leutscher-Hazelhoff 1985; Straka & Ammermüller 1991; Juusola 1993; for review, see Hardie 1985 with Hausen 1982; Maddess & Laughlin 1985 and figure 6). Computer simulations were performed to test whether this high-velocity cutoff is sufficient to ensure relative stability in an optomotor system that encodes pattern velocity up to this velocity perfectly well (unpublished results). Therefore, instead of perfect velocity sensors, velocity sensors with a cutoff at high velocities similar to the peripheral elements in the fly visual system were implemented in the input lines of the model. With this elaboration, retinal image fluctuations do not increase without bound. However, in the velocity range, in which the model optomotor system with pure velocity sensors in its input line gets unstable, the retinal image displacements are at least one order of magnitude larger (unpublished results) than those determined for the fly (figure 5 *b*, bottom diagram). This is different in the model when the cutoff of the velocity sensors is reduced to similar values as determined for the fly's optomotor system (see figure 3). Then the image fluctuations are in the same range as those generated by the fly as well as those of a model of an optomotor system with correlation-type movement detectors. This suggests that the dynamical properties of biological movement detectors, rather than the exact mechanism underlying motion detection, are responsible for the relative stability of the optomotor control system.

Although the optomotor system of the fly does not get unstable, the torque and, thus, the retinal velocity continually fluctuates. To what extent these torque fluctuations affect optomotor course stabilization may be assessed by relating the resulting displacements of the retinal image, as determined in the behavioural closed-loop experiments, to the angular spacing of the lattice points of the retinal mosaic. On the assumption that the inter-ommatidial divergence angles of the blowfly *Lucilia* lie within the range of divergence angles as found for another blowfly genus, *Calliphora* (Franceschini *et al.* 1979), the pattern displacements, on average, cover approximately four receptors. These displacements are in the same range, if related to receptor spacing, as image displacements induced by eye movements during fixation tasks in humans. These amount to at least five minutes of arc and thus shift the retinal image over about ten cones in the fovea (Barlow & Mollon 1982).As these fluctuations of the retinal image obviously do not impair stable vision in humans, it is reasonable to assume that in the fly image displacements with a similar size in terms of the retinal mosaic do not deteriorate visual orientation.

Optomotor course control as well as the visual stabilization of gaze by compensatory eye, head or body movements are of general importance in most animals including humans (Miles & Wallman 1993). During stabilization tasks, sustained fluctuations with a strong periodic component are a common feature also in eye movements of other animals such as crabs (Sandeman 1978) and monkeys (Robinson *et al.* 1986; for review, see Lisberger *et al.* 1987) and have been interpreted as a consequence of latencies in the control circuit (Sandeman 1978; Robinson *et al.* 1986; Goldreich *et al.* 1992).

Moreover, there is good evidence from electrophysiological, behavioural and psychophysical studies that movement detectors in a wide range of animals including man have very similar properties to those of insects (for review, see Borst & Egelhaaf 1989; Egelhaaf & Borst 1993). Interestingly, also in various vertebrate species the response amplitudes of motion-sensitive neurons have been found to increase with pattern velocity only within a limited dynamic range; they then reach a maximum and show a similar reduction in gain at high velocities as insect optomotor neurons (e.g. pigeon: Wolf-Oberhollenzer & Kirschfeld 1990; wallaby: Ibbotson *et al.* 1994; cat: Movshon 1975; Holub & Morton-Gibson 1981; Bisti *et al.* 1985; Baker 1990; monkey: Movshon *et al.* 1990; Lagae *et al.* 1993). Therefore, it is suggestive to speculate that the distinctive properties of biological movement detectors may quite generally affect the properties of optomotor control systems and, in particular, may play a beneficial role in ensuring their stability. Surprisingly, the characteristic dynamic properties of biological motion detectors are usually not taken into account in models of optomotor gaze stabilization. Rather, it has generally, at least implicitly, been taken for granted that the velocity of the retinal image displacements is faithfully represented in the nervous system. This statement is not entirely true: in recent studies using model simulations of smooth pursuit eye movements it has been realized that not only velocity but also acceleration may be important to explain the performance of smooth pursuit systems (Krauzliz & Lisberger 1989; Goldreich *et al.* 1992; Krauzlis 1995; Ringach 1995). In these models velocity and acceleration signals are represented in separate branches of the optomotor controller. Interestingly, the response of motion-sensitive neurons in area MT of macaque monkeys, which may be involved in the control of pursuit eye movements, does not only depend on the velocity but also on the acceleration of pattern movement (Movshon *et al.* 1990). This feature has already been described before for neurons in the optomotor pathway of the fly and can be explained by the properties of correlation-type movement detectors (Egelhaaf & Reichardt 1987). A formal analysis of the output of an array of such detectors shows that the time course of the response depends on velocity, acceleration, and to some extent on higher-order time derivatives. Therefore, it should be tested whether the monkey's performance in smooth pursuit really reflects the existence of separate velocity and acceleration pathways or rather emergent properties of its movement detection system, the output of which may depend on all these parameters in an intricate way.

In conclusion, biological movement detectors with their highly nonlinear dependence on pattern velocity are beneficial in the context of optomotor control circuits; they guarantee relative stability of the circuit while still allowing a high feedback gain that is necessary to ensure fast responses and a good compensation of disturbances.

We are grateful to J. Eikermann for help with the behavioural and electrophysiological experiments. The comments of A. Borst, V. Dürr, K. Götz, R. Kern and B. Kimmerle and, in particular, an anonymous referee, as well as a helpful discussion with J. Chahl about control systems theory are gratefully acknowledged. During part of this study A.-K. W. was financed by the Max Planck Institut für biologische Kybernetik, Tübingen, Germany. This institution also lent most of the equipment used in this study. We thank Professor K. Götz, Director of the Max Planck Institut für biologische Kybernetik, who rendered this support possible.

REFERENCES

Baker, C. L. 1990 Spatial- and temporal-frequency selectivity as a basis for velocity preference in cat striate cortex neurons. *Visual Neurosci.* **4**, 101–113.

Barlow, H. B. & Mollon, J. D. 1982 *The senses.* London, New York, Cambridge: Cambridge University Press.

Bisti, S., Carmignoto, G., Galli, L. & Maffei, L. 1985 Spatial-frequency characteristics of neurones of area 18 in the cat: Dependence on the velocity of the visual stimulus. *J. Physiol.* **359**, 259–268.

Borst, A. & Egelhaaf, M. 1987 Temporal modulation of luminance adapts time constant of fly movement detectors. *Biol. Cybern.* **56**, 209–215.

Borst, A. & Egelhaaf, M. 1989 Principles of visual motion detection. *Trends Neurosci.* **12**, 297–306.

Egelhaaf, M. 1987 Dynamic properties of two control systems underlying visually guided turning in house-flies. *J. comp. Physiol.* A **161**, 777–783.

Egelhaaf, M., Borst, A. & Reichardt, W. 1989 Computational structure of a biological motion detection system as revealed by local detector analysis in the fly's nervous system. *J. Opt. Soc. Am.* A **6**, 1070–1087.

Egelhaaf, M. & Borst, A. 1993 Movement detection in arthropods. In *Visual motion and its role in the stabilization of gaze* (ed. J. Wallman & F. A. Miles). Amsterdam: Elsevier.

Egelhaaf, M. & Reichardt, W. 1987 Dynamic response properties of movement detectors: Theoretical analysis and electrophysiological investigation in the visual system of the fly. *Biol. Cybern.* **56**, 69–87.

Fermi, G. & Reichardt, W. 1963 Optomotorische Reaktionen der Fliege *Musca domestica.* Abhängigkeit der Reaktion von der Wellenlänge, der Geschwindigkeit, dem Kontrast und der mittleren Leuchtdichte bewegter periodischer Muster. *Kybernetik* **2**, 15–28.

Franceschini, N., Münster, A. & Heurkens, G. 1979 Äquatoriales und binokulares Sehen bei der Fliege *Calliphora erythrocephala. Verh. Dtsch. Zool. Ges.* 209.

Goldreich, D., Krauzlis, R. J. & Lisberger, S. G. 1992 Effect of changing feedback delay on spontaneous oscillations in smooth pursuit eye movements of monkeys. *J. Neurophysiol.* **6**, 625–638.

Götz, K. G. 1964 Optomotorische Untersuchung des visuellen Systems einiger Augenmutanten der Fruchtfliege *Drosophila. Kybernetik* **2**, 77–92.

Hardie, R. C. 1985 Functional organization of the fly retina. In *Progress in Sensory Physiology*, vol. 5 (ed. H. Autrum, D. Ottoson, E. R. Perl, R. F. Schmidt, H. Shimazu, W. D. Willis), pp. 1–79. Berlin, Heidelberg, New York, Tokyo: Springer-Verlag.

Hausen, K. 1981 Monocular and binocular computation of motion in the lobula plate of the fly. *Verh. dt. Zool. Ges.* **74**, 49–70.

Hausen, K. 1982*a* Motion sensitive interneurons in the optomotor system of the fly. I. The horizontal cells: Structure and signals. *Biol. Cybern.* **45**, 143–156.

Hausen, K. 1982*b* Motion sensitive interneurons in the optomotor system of the fly. II. The horizontal cells: Receptive field organization and response characteristics. *Biol. Cybern.* **46**, 67–79.

Heisenberg, M. & Wolf, R. 1984 *Vision in Drosophila.* Berlin, Heidelberg, New York, Tokyo: Springer-Verlag.

Heisenberg, M. & Wolf, R. 1988 Reafferent control of optomotor yaw torque in *Drosophila melanogaster. J. comp. Physiol.* A **163**, 373–388.

Holub, R. A. & Morton-Gibson, M. 1981 Response of visual cortical neurons of the cat to moving sinusoidal gratings: Response–contrast functions and spatiotemporal interactions. *J. Neurophysiol.* **46**, 1244–1259.

Ibbotson, M. R., Mark, R. F. & Maddess, T. 1994 Spatiotemporal response properties of direction-selective neurons in the nucleus of the optic tract and dorsal terminal nucleus of the wallaby, *Macropus eugenii. J. Neurophysiol.* **72**, 2927–2943.

Juusola, M. 1993 *Contrast coding in dipteran photoreceptors. The role of phototransduction and the cell membrane.* Oulu, Acta Univ. Oulu. D 272: Doctoral Dissertation.

Kirschfeld, K. 1991 An optomotor control system with automatic compensation for contrast and texture. *Proc. R. Soc. Lond.* B **246**, 261–268.

Krauzlis, R. J. 1995 Pursuit eye movements. *The handbook of brain theory and neural networks*, 775–779 (ed. M. A. Arbib) Cambridge, MA, London: MIT Press.

Krauzlis, R. J. & Lisberger, S. G. 1989 A control systems model of smooth pursuit eye movements with realistic emergent properties. *Neur. Comput.* **1**, 116–122.

Kuo, B. C. 1991 *Automatic control systems*. Englewood Cliffs, NJ: Prentice-Hall.

Lagae, L., Raiguel, S. & Orban, G. A. 1993 Speed and direction selectivity of macaque middle temporal neurons. *J. Neurophysiol.* **69**, 19–39.

Land, M. F. 1992 Visual tracking and pursuit: Humans and arthropods compared. *J. Insect. Physiol.* **38**, 939–951.

Laughlin, S. 1981 Neural principles in the peripheral visual system of invertebrates. In *Handbook of Sensory Physiology*, vol. VII/6B, (ed. H. Autrum), pp. 133–280. Berlin, Heidelberg, New York: Springer-Verlag.

Leutscher-Hazelhoff, J. T. 1975 Linear and non-linear performance of transducer and pupil in *Calliphora* retinula cells. *J. Physiol.* **246**, 333–350.

Lisberger, S. G., Morris, E. J. & Tychsen, L. 1987 Visual motion processing and sensory–motor integration for smooth pursuit eye movements. *Ann. Rev. Neurosci.* **10**, 97–129.

Maddess, T. & Laughlin, S. B. 1985 Adaptation of the motion-sensitive neuron H1 is generated locally and governed by contrast frequency. *Proc. R. Soc. Lond.* B **225**, 251–275.

Mayer, M. 1989 *Räumliche und zeitliche Integration von Bewegungsinformation im visuellen Flugsystem von Drosophila melanogaster. Modellentwicklung auf der Grundlage von Verhaltens-Versuchen.* Universität Würzburg: Doctoral Dissertation.

Miles, F. A. & Wallman, J. (eds) 1993 *Visual motion and its role in the stabilization of gaze.* Amsterdam, London, New York: Elsevier.

Movshon, J. A. 1975 The velocity tuning of single units in cat striate cortex. *J. Physiol.* **24**, 445–468.

Movshon, J. A., Lisberger, S. G. & Krauzlis, R. J. 1990 Visual cortical signals supporting smooth pursuit eye movements. *Cold Spring Harb. Symp. Quant. Biol.* LV, pp. 707–716.

Pick, B. & Buchner, E. 1979 Visual movement detection under light- and dark-adaptation in the fly, *Musca domestica. J. comp. Physiol.* A **134**, 45–54.

Reichardt, W. 1973 Musterinduzierte Flugorientierung. Verhaltens-Versuche an der Fliege *Musca domestica. Naturwissenschaften* **60**, 122–138.

Reichardt, W. & Poggio, T. 1976 Visual control of orientation behaviour in the fly. Part I. A quantitative analysis. *Quart. Rev. Biophys.* **9**, 311–375.

Ringach, D. L. 1995 A 'tachometer' feedback model of smooth pursuit eye movements. *Biol.Cybern.* **73**, 561–568.

Robinson, D. A., Gordon, J. L. & Gordon, S. E. 1986 A model of the smooth pursuit eye movement system. *Biol. Cybern.* **55**, 43–57.

Ruyter van Steveninck, R. de, Zaagman, W. H. & Mastebroek, H. A. K. 1986 Adaptation of transient responses of a movement-sensitive neuron in the visual system of the blowfly, *Calliphora erythrocephala. Biol. Cybern.* **54**, 223–236.

Sandeman, D. C. 1978 Eye-scanning during walking in the crab *Leptocrapsus variegatus. J. comp. Physiol.* **124**, 249–257.

Straka, H. & Ammermüller, J. 1991 Temporal resolving power of blowfly visual system: effects of decamethonium and hyperpolarization on responses of laminar monopolar neurons. *J. comp. Physiol.* A **168**, 129–139.

Varjú, D. 1973 Übertragungseigenschaften im Auswertesystem für das Bewegungssehen. *Nova Acta Leopoldina* (ed. J. Scharf, B. Luecken, & J. A. Barth), Leipzig.

Warzecha, A.-K. 1994 *Reliability of neuronal information processing in the motion pathway of the blowflies Calliphora erythrocephala and Lucilia cuprina.* Universität Tübingen: Doctoral Dissertation.

Warzecha, A.-K., Egelhaaf, M. & Borst, A. 1993 Neural circuit tuning fly visual neurons to motion of small objects. I. Dissection of the circuit by pharmacological and photoinactivation techniques. *J. Neurophysiol.* **69**, 329–339.

Wolf, R. & Heisenberg, M. 1990 Visual control of straight flight in *Drosophila melanogaster. J. comp. Physiol.* A **167**, 269–283.

Wolf-Oberhollenzer, F. & Kirschfeld, K. 1990 Temporal frequency dependence in motion-sensitive neurons of the accessory optic system of the pigeon. *Naturwissenschaften* **77**, 296–298.

Young, L. R. 1971 Pursuit eye tracking movements. *The control of eye movements* (ed. P. Bach-Y-Rita, C. C. Collins, & J. E. Hyde), pp. 429–444. New York: Academic Press.

Received 6 September 1995; accepted 18 April 1996